Original Article

Microstructured Porous Capacitive Bio-pressure Sensor Using Droplet-based Microfluidics

Mohammadmahdi Eskandarisani[1]*, Mahdi Aliverdinia[1]*, Vahid Mollania Malakshah[1], Shaghayegh Mirhosseini[2], Mahdi Moghimi Zand[1]

[1]School of Mechanical Engineering, [2]School of Electrical and Computer Engineering, College of Engineering, University of Tehran, Tehran, Iran
**These authors contributed equally as the first author*

Abstract

Background: Devices that mimic the functions of human skin are known as "electronic skin," and they must have characteristics like high sensitivity, a wide dynamic range, high spatial homogeneity, cheap cost, wide area easy processing, and the ability to distinguish between diverse external inputs. **Methods:** This study introduces a novel approach, termed microfluidic droplet-based emulsion self-assembly (DMESA), for fabricating 3D microstructured elastomer layers using polydimethylsiloxane (PDMS). The method aims to produce accurate capacitive pressure sensors suitable for electronic skin (e-skin) applications. The DMESA method facilitates the creation of uniform-sized spherical micropores dispersed across a significant area without requiring a template, ensuring excellent spatial homogeneity. **Results:** Micropore size adjustment, ranging from 100 to 600 μm, allows for customization of pressure sensor sensitivity. The active layer of the capacitive pressure sensor is formed by the three-dimensional elastomer itself. Experimental results demonstrate the outstanding performance of the DMESA approach. It offers simplicity in processing, the ability to adjust performance parameters, excellent spatial homogeneity, and the capability to differentiate varied inputs. Capacitive pressure sensors fabricated using this method exhibit high sensitivity and dynamic amplitude, making them promising candidates for various e-skin applications. **Conclusion:** The DMESA method presents a highly promising solution for fabricating 3D microstructured elastomer layers for capacitive pressure sensors in e-skin technology. Its simplicity, performance adjustability, spatial homogeneity, and sensitivity to different inputs make it suitable for a wide range of electronic skin applications.

Keywords: *Droplet, electronic skin, flexible sensor, health-care monitoring, microfluidic capacitive pressure sensor*

Submitted: 06-Jun-2023 **Revised:** 15-Nov-2023 **Accepted:** 11-Dec-2023 **Published:** 02-Jul-2024

Introduction

Devices that mimic the intricate functions of human skin, commonly referred to as "e-skin," have garnered significant attention in recent years.[1-6] It is typically embedded with various sensors, actuators, and electronic components to detect and respond to physical stimuli such as pressure, temperature, and touch. E-skin technology aims to bridge the gap between the digital and physical worlds by providing a means for the seamless integration of electronic devices with the human body or other objects. These remarkable creations find extensive utility in various fields, particularly in the realm of wearable technology for health-care applications.[7-9] The integration of e-skin into this domain has brought about revolutionary advancements in areas such as pressure-sensitive touch displays,[2,10] human-computer interfaces,[11,12] prostheses,[9,13,14] and user-friendly robotics,[5,15-18] expanding the possibilities of human-machine interactions.

One of the crucial aspects of e-skin design is the ability to replicate the dynamic characteristics of human skin with utmost accuracy. To achieve this, e-skin must exhibit a wide dynamic amplitude, capable of sensing pressures up to 105 pascals. This exceptional range allows e-skin to capture subtle and forceful touches alike, enabling precise and nuanced tactile feedback. Furthermore, e-skin should possess remarkable spatial resolution, enabling it to discern fine details and textures on the surface it interacts with. This high resolution is paramount in applications where intricate sensory perception is crucial, such as medical diagnostics and prosthetic limb control. In addition, e-skin must maintain

How to cite this article: Eskandarisani M, Aliverdinia M, Malakshah VM, Mirhosseini S, Zand MM. Microstructured porous capacitive bio-pressure sensor using droplet-based microfluidics. J Med Signals Sens 2024;14:14.

Address for correspondence:
Prof. Mahdi Moghimi Zand, School of Mechanical Engineering, University of Tehran, Tehran, Iran.
E-mail: mahdimoghimi@ut.ac.ir

Access this article online

Website: www.jmssjournal.net

DOI: 10.4103/jmss.jmss_24_23

Quick Response Code:

fine homogeneity across its entire surface, ensuring consistent and reliable sensing capabilities. Electronic skin should also have the same ability as human skin to discern between diverse environmental inputs, including temperature, pressure, and closeness (human skin accomplishes this through hair follicles).[19-21] This uniformity allows e-skin to faithfully reproduce the diverse characteristics of human skin, ensuring an immersive and realistic user experience.

In the pursuit of improving the pressure sensitivity of e-skin, one commonly employed technique involves microstructuring the active layer. By introducing microstructures into the active layer, the e-skin can achieve enhanced performance and more accurate pressure-sensing capabilities. Among the various methods used for microstructuring, mold casting has emerged as a highly popular and effective technique.[19,22-26]

Mold casting involves creating a mold with precise microstructural features, which is then used to imprint the desired pattern onto the active layer of the e-skin. This process has been particularly successful in enhancing the performance of capacitive pressure sensors integrated into e-skin.

A nanofiber-based electronic skin with extremely high-pressure sensitivity and three-dimensional (3D) conformability was created by Zhong *et al*.[27] and constructed by interconnecting two elastically structured nanofibrous membranes. The patterned membrane is quickly created by pouring conductive nanofiber ink into a silicon mold to create a variety of protuberances that resemble semi-spheroids. The protuberances made of interlaced elastic POE (elastic polyolefin elastomer) nanofibers and PPy/PVA-co-PE nanofibers (polypyrrole (PPy) conformally coated Poly (ethylene terephthalate) PVA-co-PE nanofibers) nanofibers have a high sensitivity for pressure sensing thanks to their adjustable effective elastic modulus, which can capture a variety of strains and stresses. With a detection limit as low as roughly 1.3 Pa, this electronic skin-like sensor has an ultra-high sensitivity (1.24 kPa) below 150 Pa. The RGB-LED light and pixelated sensor array are then put together into a circuit that demonstrates the viability of visual-spatial pressure sensing.

Park *et al*.[28] developed the successful integration of a triboelectric nanogenerator into an electronic skin, allowing for both biomechanical energy harvesting and self-pressure sensing capabilities, all without the need for an external power source. To achieve this, they combined PTFE-molded (Polytetra-fluoroethylene) micro-patterned polydimethylsiloxane (PDMS) with a conductive yarn, resulting in an e-skin that possesses remarkable flexibility, elasticity, high sensitivity, and perfect stability.

However, it is important to note that mold casting does have a limitation when it comes to the thickness of the microstructured layer. The thickness achievable through this technique typically ranges from only a few to a few hundred microns. Based on factors such as the ratio of the height to the width of the microstructures (the aspect ratio) and the depth of etching for the microstructural features on the mold.[24,25] These limitations stem from the practical constraints of the mold fabrication process and the subsequent transfer of the microstructures onto the e-skin's active layer.

While mold casting offers significant benefits in terms of improved pressure sensitivity, its thickness restrictions can sometimes pose challenges, especially in applications where thicker or more complex microstructures are desired. As a result, numerous pressure sensors possess a limited dynamic range, and their responses tend to saturate at pressures exceeding a few tens of kilopascals.[22,24] For e-skin applications, which need a wide dynamic range of several to hundred kilopascals, this might be a limiting issue.[4] Researchers and engineers are actively exploring alternative methods and innovative approaches to overcome these limitations and expand the range of achievable microstructural designs in e-skin technology.

This problem can be addressed through various methods. One approach involves the random mixing of aqua phases and oil to create an emulsion, followed by the removal of solvents. Another method, explored by a few researchers, entails using 3D templates made of materials like polystyrene beads, nickel foam, or sugar. These templates are filled with the active material, and then, the template is etched away.[29-36]

Kwon *et al*.[31] have developed a flexible and wearable pressure sensor with a wide tactile pressure range in line with the gigantic piezocapacitive influence of a 3D microporous dielectric elastomer. Their piezocapacitive pressure sensor is extremely deformable by even very tiny quantities of pressure, resulting in a huge enhancement in its sensitivity because of the existence of micropores inside the elastomeric dielectric layer. In addition, the effective dielectric constant rises due to the progressive closing of micropores under compression, increasing the sensitivity of the sensor. Compared to previously identified micro-/nanostructured sensing materials, the 3D microporous dielectric layer with serially stacked springs of elastomer bridges can withstand a substantially larger pressure range. In light of this, their pressure sensor demonstrated remarkable performance with ultra-high-sensitivity of 0.601 kPa-1 in a low-pressure domain (<5 kPa) and a large dynamic range of 0.1 Pa-130 kPa, which is suitable for typical tactile pressure ranges without suffering a substantial loss in sensitivity.

Li *et al*.[37] introduced a novel fabrication method for porous PDMS. The method combines structured molding, micro-region fusion, and vacuum-assisted infiltration using salt particles as porogen. Although the procedure is quick and easy, independent of the pore size distribution,

it significantly improves pore interconnectivity and salt residue in the final porous PDMS samples. The technique also makes it possible to create porous PDMS samples with a variety of 3D structural contours, emphasizing its potent structurization potential, which is rarely addressed by other techniques. The technique produces effective 3D structure construction, improved pore interconnectivity, and less salt residue by integrating structured molding, micro-region fusing, and vacuum-assisted infiltration. The efficacy and adaptability of the suggested technology are demonstrated by experimental demonstrations that illustrate the successful production of porous PDMS samples with various pore size distributions and structural contours. The fabrication of a capacitive pressure sensor, which has increased sensing sensitivity compared to a planar equivalent, further validates the application advantage afforded by the structurization capabilities of porous PDMS.

However, these existing procedures have certain limitations. First, they can be somewhat expensive, making them less suitable for low-cost, large-area devices. In addition, they often result in microstructures with arbitrary shapes and sizes, which limits their spatial uniformity, especially in situations where precise taxel accuracy is essential.[34,36] Another challenge is the difficulty in controlling the shape and the microstructures' size, which affects the tunability of system efficiency. Hence, it is necessary to develop a simple and affordable template-free method that can generate 3D microstructures with uniform sizes and variable feature sizes while ensuring significant area homogeneity. A highly promising technique, microfluidics, offers a range of biomedical applications, including cell separation[38-41] and DNA sequencing.[42-45] The utilization of microfluidic devices opens up numerous opportunities in various fields, such as production of monodisperse double emulsions,[46,47] particle focusing,[48] and particle separation.[49-51]

In this study, we provide a novel microfluidic droplet-based emulsion self-assembly (DMESA) method for fabricating a 3D microstructured elastomer PDMS layer that might be utilized to produce accurate capacitive pressure sensors for e-skin applications. The DMESA method presents a unique and advantageous approach for the manufacturing of 3D microstructured elastomer layers when compared to the other techniques discussed in the additional papers. Unlike traditional 3D printing with PDMS, DMESA eliminates the need for extended curing times associated with liquid polymer precursors, offering a more efficient and streamlined process. In contrast to the method involving flexible capacitive pressure sensors with porous PDMS, DMESA showcases outstanding spatial homogeneity, enabling the creation of uniform-sized spherical micropores distributed across a substantial area. Furthermore, DMESA's innovation lies in utilizing the elastomer itself as the active layer, resulting in the successful fabrication of capacitive pressure sensors with high sensitivity and dynamic amplitude. This approach combines exceptional performance, the ability to distinguish varying inputs, and straightforward processing, making it a highly promising solution across a broad spectrum of electronic skin applications. In comparison to methods concerning porous PDMS sponges or porous PDMS fabrication with salt particles, DMESA's specialization in pressure sensor creation ensures tailored solutions for e-skin technology, with an emphasis on sensitivity control and spatial uniformity in microstructured elastomer layers.

The DMESA method may create spherical micropores of uniform size that are evenly dispersed across a substantial area without the requirement for a template, resulting in excellent spatial homogeneity. The micropore size, which ranges from 100 to 600 μm, may be easily changed to change the sensitivity of the pressure sensor. Capacitive pressure sensors with sensitivity as high as 0.62 kPa-1 and a dynamic amplitude as high as 100 kPa were made using the 3D elastomer itself as the active layer. Our approach is quite distinctive and looks to be highly encouraging for a broad spectrum of prospective electronic skin applications because to these instances of straightforward processing, performance adjustment, excellent spatial homogeneity, and differentiation of varied inputs.

This work is an extended version of our previous work which was published in ICBME 2022 (microstructured droplet-based porous capacitive pressure sensor). Herein, we have modified the previous work with explaining more about the concepts and ideas in this field and discussing more examples of similar works in the state of art. We have also compared our results with other papers in order to increase the credit of validating our work. Fabricating a structure with enhancing the precision of droplet generation would be convenient for future works.

Fabrication Methodology

To create microchips with accurate features, soft contact lithography techniques were used. The process began using SU-8 2050 to create a 100 μm thick mold on a silicon wafer substrate. This mold served as the template for the microchip's structure. The microchip design included various components to facilitate its functionality. Only one outlet was incorporated, along with a flow-focusing junction measuring 500 μm in size. The junction featured a vertical angle to enable droplet production. Two inlets were provided to accommodate the scattered and continuous phases of the system. In addition, an expanding chamber was positioned before the outlet to slow down the advancing speed of the microdroplets, allowing them to be held in place for imaging purposes. To create the channel within the microchip, PDMS was cast onto the mold. This process involved pouring the PDMS material onto the mold and using a hotplate to cure it. A 10:1 mixture of PDMS monomer and curing agent was applied, and the curing process took place at a temperature of 75°C for 30 min.

Once cured, the finished PDMS structure was prepared by using a 1 mm punch to create output and input ports, facilitating the flow of fluids through the microchip. Aluminum electrodes were employed as the bottom and top components of the microchip structure. These electrodes played a crucial role in the overall functionality of the device. The generation of deionized (DI)-water droplets and PDMS involved transferring them to a simple rectangular mold using a tube. Subsequently, the contents within the mold were subjected to heat on a hotplate for 2 h at a temperature of 90°. This heat treatment induced a phase change in the PDMS material, causing it to solidify and form the desired structure. Simultaneously, the heat also evaporated the water droplets, leaving behind holes in the structure. The droplets required for the experiment were generated using a focusing microchannel with a 200 μm junction. This specific setup allowed for precise control and manipulation of the droplets during the experimental process. The production of deionized water droplets within silicone oil through a flow-focusing microchannel is shown in figure 1.

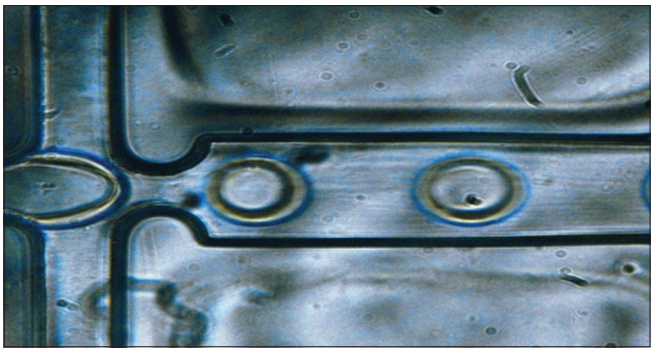

Figure 1: The production of deionized water droplets within silicone oil through a flow-focusing microchannel

Results and Discussion

In order to assess the impact of various parameters on droplets, we conducted experiments to manipulate the disperse phase's capillary number, represented by $(\frac{\mu_d \times \mu_d}{\sigma})$. We aimed to investigate how this parameter affects the droplet size, the distance between them, and the frequency of droplet production. To achieve this, it was necessary to transform the values into dimensionless form, which was accomplished by introducing the Strouhal number, given by $(\frac{f \times l}{\mu_d})$, to represent frequency. In addition, the longitudinal dimensions were made dimensionless by dividing them by the orifice width, denoted as $L_{Oriffice}$. The outcomes of these investigations are depicted in Figures 2-4.

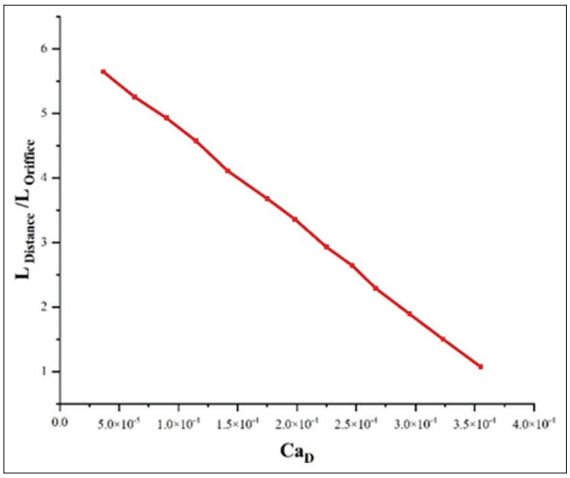

Figure 2: Influence of the Ca number of the dispersed phase on droplet size

Figure 2 illustrates the impact of the capillary number of the dispersed phase on droplet size. It shows that the size of formed droplets increases linearly up to approximately $Ca_D < 3 \times 10^{-4}$. Beyond this threshold ($Ca_D > 3 \times 10^{-4}$), the size of the droplets remains constant, indicating a saturation point. In Figure 3, the relationship between the capillary number of the dispersed phase and the distance between droplets is demonstrated. It reveals that as the capillary number increases, the distance between the droplets decreases linearly. This suggests that higher capillary numbers lead to a more compact arrangement of droplets. Figure 4 focuses on the effect of the capillary number of the dispersed phase on the droplet production frequency, represented by St_D. The results indicate that as the capillary number increases, the droplet production frequency (St_D) decreases. This implies that higher capillary numbers correspond to a reduced rate of droplet production.

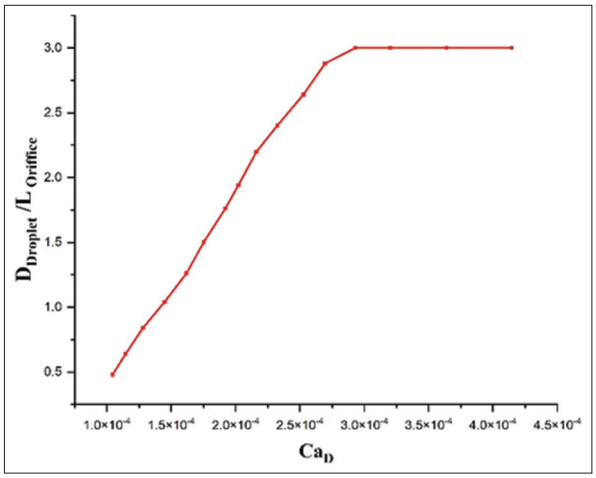

Figure 3: The impact of the Ca number of the dispersed phase on the spacing between two droplets

These findings from the experiments provide valuable insights into the relationship between the capillary number of the dispersed phase and various droplet characteristics. By analyzing [Figures 2-4], it becomes evident that manipulating the capillary number can significantly influence droplet size, inter-droplet distance, and droplet production frequency.

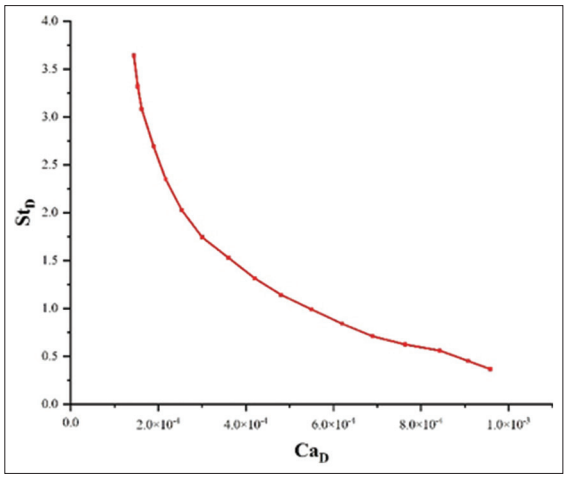

Figure 4: The impact of the Ca number of the dispersed phase on the droplet generation frequency (St_D)

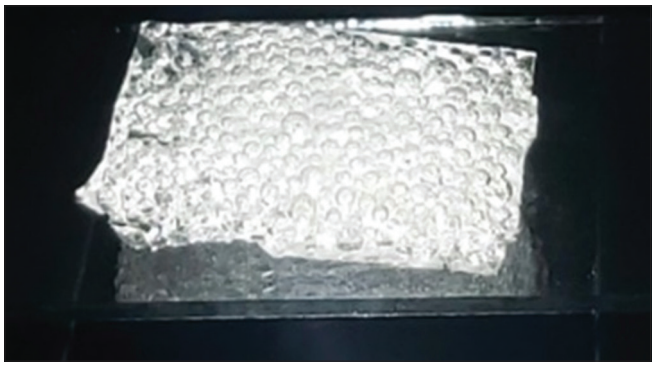

Figure 6: Droplet based porous structure

The process of gathering DI water droplets leads to the formation of tightly packed two-dimensional lattices. These lattices then stack up vertically, resulting in the creation of a tightly packed 3D structure. This 3D structure is characterized by its closely arranged microstructures, which contribute to its unique properties. During the curing process of the PDMS, the DI water within the droplets gradually evaporates. As the water evaporates, it leaves behind a 3D microstructured PDMS that maintains a uniform micropore dimensions. To validate the structural integrity and stability of the 3D microporous structure during the evaporation process, scannable optical microscope images were captured. The 3D microporous structure's ability to keep its form without collapsing as water evaporates is related to PDMS's gas permeability, according to scannable optical microscope images. Different sizes of generated droplets are shown in figure 5 and the whole droplet based porous structure is depicted in figure 6.

We have also tested two structures in addition to the droplet-based method; first using sugar grains and second one with salt grains. The process of making the aforementioned structures starts with mixing them with PDMS solution. Then, we bake them in the oven at 90°C for 20 min. After the baking process, we put the structures

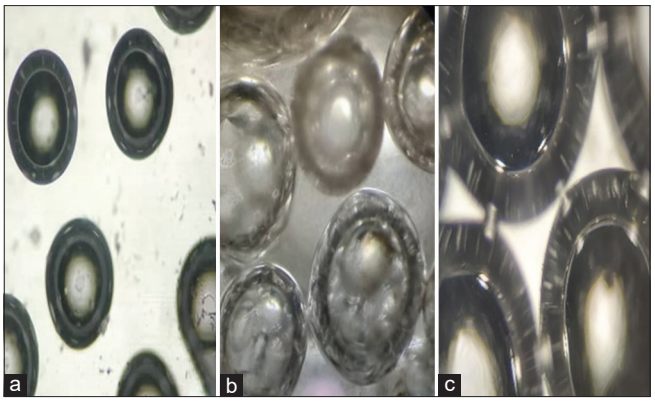

Figure 5: Microscopic images of (a) 100 µm droplets, (b) 200 µm droplets and (c) 400 µm droplets

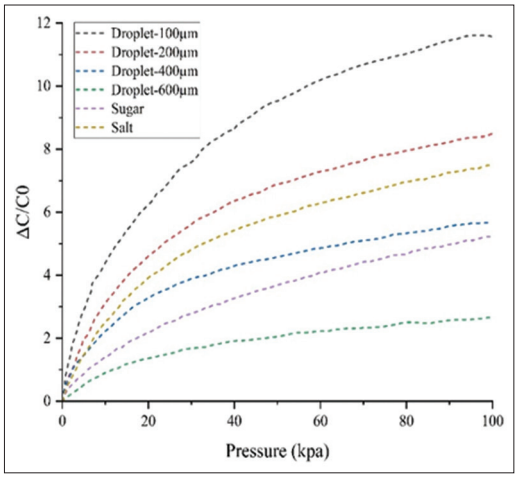

Figure 7: Graphs displaying the relative capacitance change in relation to pressure for samples with different micropore sizes (Y-axis is with a scale of 100th for relative capacitance change)

in DI water (totally drowned). After 48 h, the sugar grains and salt grains are dissolved in DI water and the porous structure is complete. In the end, putting them exposed to free air will make them dry and ready to use. The sugar and salt grains make micropores with approximately 500 and 300 µ, respectively.

The analysis of the curves depicting relative capacitance change as a function of pressure for samples with diverse micropore sizes indicates that the sensitivity of the capacitive pressure sensors is influenced by the size of the micropores and the applied pressure. By examining [Figure 7], it can be observed that the relative capacitance variation (ΔC/Co) increases as the pressure range is expanded for each of the six samples created with different pore sizes (sugar grain size, salt grain size, 100, 200, 400, and 600 µm droplet sizes).

In comparison to the sample with lesser porosity, the sample with higher porosity also exhibits a reduced compressive modulus. The following can be used to explain this distinction. A porous system experiences buckling, which is an outward deflection, in the thin rows

between two pores. Due to Euler's critical load, the force at which buckling occurs is inversely linked to the width of the thin row between the holes. As buckling transpires at a lower pressure due to the longer row of larger holes, the sample with larger pores undergoes greater strain than the specimen with smaller pores under equivalent pressure conditions. For all samples, the sensitivity was uniformly poor at low pressures and gradually decreased as pressure increased. Intriguingly, as the size of micropores increased from 100 μm to 600 μm, ΔC/Co at 100 kPa increased by around four times. In addition, the sensitivity of the devices enhanced with larger pore sizes, and differences in sensitivities were more pronounced in the lower-pressure area and steadily diminished with rising pressure.

Based on the microstructured arrangement, it is evident that the relative capacitance (ΔC/Co) values of the four samples are close to each other at low-pressure ranges. However, at higher pressure ranges, significant differences in the relative capacitance (ΔC/Co) values can be observed, and overall, the relative capacitance (ΔC/Co) values are higher for samples with larger micropores (100, 200, 400, and 600 μm) throughout the pressure range. In the sample with 100 μm micropores, the relative capacitance increases rapidly upon the application of pressure, indicating that smaller micropores require less pressure to reach their maximum capacitance. Conversely, in the sample with 600 μm micropores, the relative capacitance increases more slowly and reaches a lower value than the other samples. This trend suggests that larger micropores require higher pressure to achieve their maximum capacitance. For testing the fabricated device, we put the sensor on human fist and monitor the changes of capacitance over time. Figure 8 shows the change in relative capacitance over time, demonstrating real-time monitoring of human movements with both an open and closed fist.

At the same pressure, the specimen with pores of 200 μm does not buckle, while the specimen with pores of 600 μm displays collapsed pores as a result of buckling. Under extreme pressure, the pores in both samples will close. The sensitivity of specimens with diverse micropore sizes will, therefore, begin to merge when the structural influence of the various pore sizes is lost.

Based on the information presented in Figure 7, it is shown that the fabricated sensor is suitable for pressure ranges from 0 to 100 kilopascals (kPa). To provide a point of comparison, it is worth noting that a separate research group[52,53] pursued a different approach to create a PDMS structure with porosity. This method involved using DI water evaporation. While this technique resulted in an economically viable flexible pressure sensor based on a porous PDMS structure, it exhibits constraints in terms of its suitability for low-pressure scenarios and demonstrates less than ideal linearity when exposed to wide-ranging pressure conditions. Furthermore, there is another study[37] that employs an innovative methodology, incorporating structured molding, micro-region fusion, and vacuum-assisted infiltration, with salt particles serving as a porogen. However, it is important to recognize that this method is also most effective in low-pressure situations.

For comparing our result in relative capacitance change and, therefore, its effectiveness, we have considered Li *et al*.'s[37] work to compare the relative capacitance change as a function of pressure. For having a precise comparison between the aforementioned results and ours, we considered the most effective structure in our experiments, which was 100 μm pore size and droplets. As it is depicted in Figure 9, Li *et al*.[37] compared different shapes of porous structures. First, the planar-shaped structure, which is pretty similar to our work. Then, the dome-shaped structure showed a better result in relative capacitance change. They also had a 300–450 μm pore size distribution in their structure. It can be seen that our structure has a slightly better response to pressure compared to Li *et al*. dome-shaped structure. Therefore, it is more sensitive under different loads of pressure.

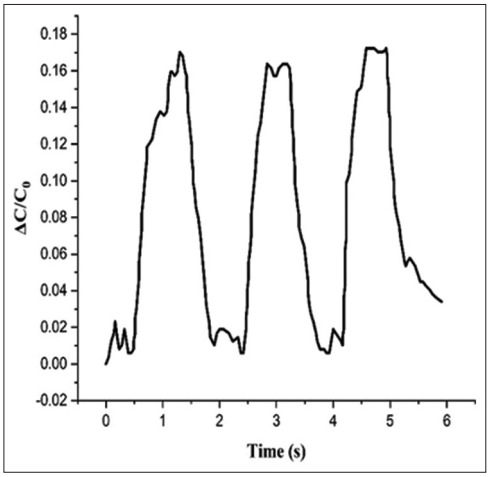

Figure 8: Graphs illustrating the change in relative capacitance over time, demonstrating real-time monitoring of human movements with both an open and closed fist

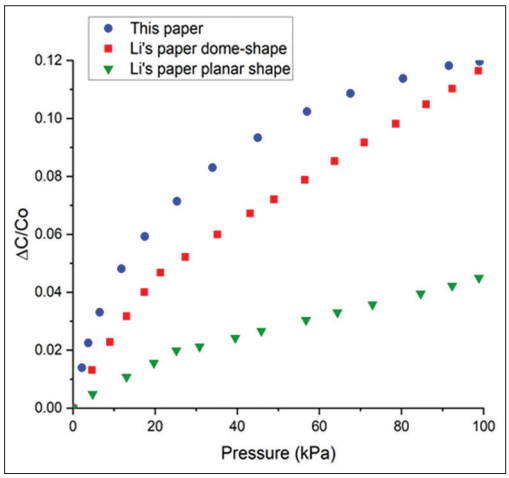

Figure 9: Curves of relative capacitance change as a function of pressure comparing to Li et al.[37] results

In summary, the analysis reveals that the size of micropores in the capacitive pressure sensors affects their sensitivity and response to pressure. Smaller micropores exhibit a higher sensitivity and reach maximum capacitance at lower pressures, while larger micropores exhibit a lower sensitivity and require higher pressures to reach their maximum capacitance.

Other vital attributes of e-skin applications encompass precise spatial resolution and uniformity. Fine spatial resolution refers to the ability of the e-skin to accurately detect and distinguish between small changes in the contact region. To achieve this, it is important that only the area directly in contact with an object or surface is compressed while the surrounding area remains unconstrained. By compressing only the contact region, the e-skin can effectively capture and analyze the subtle variations in capacitance or pressure that occur during interactions. This allows for precise tracking and recognition of touch or pressure patterns, enabling more detailed and accurate feedback to be provided.

Homogeneity is another important aspect of e-skin applications. It refers to the uniformity of the sensing capabilities across the entire surface of the e-skin. The e-skin should exhibit consistent sensitivity and response characteristics regardless of the specific location being touched or pressed. This ensures reliable and consistent performance, enabling reliable detection and interpretation of tactile information. Both fine spatial resolution and homogeneity are essential for e-skin applications in various fields, such as robotics, prosthetics, and virtual reality. These characteristics enable the e-skin to mimic the sensitivity and responsiveness of human skin, allowing for natural and intuitive interactions with the environment.

Conclusion

The study introduced a new microfluidic DMESA method for fabricating 3D microstructured elastomer layers in the context of capacitive pressure sensors for e-skin applications. The DMESA approach demonstrated excellent performance in terms of spatial homogeneity, simplicity in processing, and the ability to adjust sensitivity by controlling micropore size. The fabricated capacitive pressure sensors exhibited high sensitivity and dynamic amplitude, showcasing the potential for accurate pressure detection. The findings shed light on the influence of micropore size and applied pressure on the sensitivity and response of the sensors. In addition, important characteristics such as fine spatial resolution and homogeneity were highlighted as essential for e-skin applications. Overall, the presented method shows promise for various electronic skin applications, offering a distinctive approach with straightforward processing, performance customization, and excellent spatial homogeneity to enable reliable and precise tactile sensing capabilities.

Financial support and sponsorship

Nil.

Conflicts of interest

There are no conflicts of interest.

References

1. Hammock ML, Chortos A, Tee BC, Tok JB, Bao Z. 25th anniversary article: The evolution of electronic skin (e-skin): A brief history, design considerations, and recent progress. Adv Mater 2013;25:5997-6038.
2. Miyamoto A, Lee S, Cooray NF, Lee S, Mori M, Matsuhisa N, *et al.* Inflammation-free, gas-permeable, lightweight, stretchable on-skin electronics with nanomeshes. Nat Nanotechnol 2017;12:907-13.
3. Schwartz G, Tee BC, Mei J, Appleton AL, Kim DH, Wang H, *et al.* Flexible polymer transistors with high pressure sensitivity for application in electronic skin and health monitoring. Nat Commun 2013;4:1859.2.
4. Zang Y, Zhang F, Di CA, Zhu D. Advances of flexible pressure sensors toward artificial intelligence and health care applications. Mater Horiz 2015;2:140-56.
5. Someya T, Sekitani T, Iba S, Kato Y, Kawaguchi H, Sakurai T. A large-area, flexible pressure sensor matrix with organic field-effect transistors for artificial skin applications. Proc Natl Acad Sci U S A 2004;101:9966-70.
6. Ramuz M, Tee BC, Tok JB, Bao Z. Transparent, optical, pressure-sensitive artificial skin for large-area stretchable electronics. Adv Mater 2012;24:3223-7.
7. Kim J, Lee M, Shim HJ, Ghaffari R, Cho HR, Son D, *et al.* Stretchable silicon nanoribbon electronics for skin prosthesis. Nat Commun 2014;5:5747.
8. Zeng W, Shu L, Li Q, Chen S, Wang F, Tao XM. Fiber-based wearable electronics: A review of materials, fabrication, devices, and applications. Adv Mater 2014;26:5310-36.
9. Rogers JA, Someya T, Huang Y. Materials and Mechanics for Stretchable Electronics; 2010. doi: 10.1126/science.1182383.
10. Sadasivuni KK, Kafy A, Zhai L, Ko HU, Mun S, Kim J. Transparent and flexible cellulose nanocrystal/reduced graphene oxide film for proximity sensing. Small 2015;11:994-1002.
11. Bi S, Jin W, Han X, Metts J, Ostrosky AD, Lehotsky J. Flexible pressure visualization equipment for human computer interaction. Mater Today Sustain 2023;21:351-62. [doi: 10.1016/j.mtsust.2023.100318].
12. Jiang S, Li L, Xu H, Xu J, Gu G, Shull PB. Stretchable e-Skin patch for gesture recognition on the back of the hand. IEEE Transact on Indust Electron 2020;67:647-57.
13. Dos Santos A, Pinela N, Alves P, Santos R, Farinha R, Fortunato E, *et al.* E-Skin bimodal sensors for robotics and prosthesis using PDMS molds engraved by laser. Sensors (Basel) 2019;19:899.
14. Iskarous MM, Thakor NV. E-Skins: Biomimetic Sensing and Encoding for Upper Limb Prostheses. Proc IEEE 2019;107:2052-64.
15. Trivedi D, Rahn CD, Kier WM, Walker ID. Soft robotics: Biological inspiration, state of the art, and future research. Appl Bionics Biomech 2008;5:99-117.
16. Webb RC, Bonifas AP, Behnaz A, Zhang Y, Yu KJ, Cheng H, *et al.* Ultrathin conformal devices for precise and continuous thermal characterization of human skin. Nat Mater 2013;12:938-44.

17. Pignanelli J, Schlingman K, Carmichael TB, Rondeau Gagné S, Ahamed MJ. A comparative analysis of capacitive-based flexible PDMS pressure sensors. Sens Actuators Phys 2019;285:427-36.
18. Munirathinam K, Park J, Jeong YJ, Lee DW. Galinstan based flexible microfluidic device for wireless human sensor applications. Sens Actuators Phys 2020;315:594-603. [doi: 10.1016/j. sna. 2020.112344].
19. Yamamoto Y, Harada S, Yamamoto D, Honda W, Arie T, Akita S, *et al.* Printed multifunctional flexible device with an integrated motion sensor for health care monitoring. Sci Adv 2016;2:e1601473.
20. Sarwar MS, Dobashi Y, Preston C, Wyss JK, Mirabbasi S, Madden JD. Bend, stretch, and touch: Locating a finger on an actively deformed transparent sensor array. Sci Adv 2017;3:e1602200.
21. Hua Q, Sun J, Liu H, Bao R, Yu R, Zhai J. Skin-inspired highly stretchable and conformable matrix networks for multifunctional sensing. Nat Commun 2018;9:169-82. [doi: 10.1038/s41467-017 02685-9].
22. Tee BC, Chortos A, Dunn RR, Schwartz G, Eason E, Bao Z. Tunable flexible pressure sensors using microstructured elastomer geometries for intuitive electronics. Adv Funct Mater 2014;24:5427-34.
23. Mannsfeld SC, Tee BC, Stoltenberg RM, Chen CV, Barman S, Muir BV, *et al*. Highly sensitive flexible pressure sensors with microstructured rubber dielectric layers. Nat Mater 2010;9:859-64.
24. Choong CL, Shim MB, Lee BS, Jeon S, Ko DS, Kang TH, *et al.* Highly stretchable resistive pressure sensors using a conductive elastomeric composite on a micropyramid array. Adv Mater 2014;26:3451-8.
25. Pan L, Chortos A, Yu G, Wang Y, Isaacson S, Allen R, *et al.* An ultra-sensitive resistive pressure sensor based on hollow-sphere microstructure induced elasticity in conducting polymer film. Nat Commun 2014;5:3002.
26. Sani MM, Aliverdinia M, Javidi R, Mirhosseini S, Zand MM. Microstructured droplet based porous capacitive pressure sensor. In: 2022 29th National and 7th International Iranian Conference on Biomedical Engineering (ICBME). IEEE; 2022. p. 321-4:
27. Zhong W, Liu Q, Wu Y, Wang Y, Qing X, Li M, *et al*. A nanofiber based artificial electronic skin with high pressure sensitivity and 3D conformability. Nanoscale 2016;8:12105-12.
28. Park J, Kim D, Kim YT. Soft and transparent triboelectric nanogenerator based E skin for wearable energy harvesting and pressure sensing. Nanotechnology 2021;32:271-80. [doi: 10.1088/1361-6528/ac0c3f].
29. Choi SJ, Kwon TH, Im H, Moon DI, Baek DJ, Seol ML, *et al*. A polydimethylsiloxane (PDMS) sponge for the selective absorption of oil from water. ACS Appl Mater Interfaces 2011;3:4552-6.
30. Rinaldi A, Tamburrano A, Fortunato M, Sarto MS. A flexible and highly sensitive pressure sensor based on a PDMS foam coated with graphene nanoplatelets. Sensors (Switzerland) 2016;16:119-31. [doi: 10.3390/s16122148].
31. Kwon D, Lee TI, Shim J, Ryu S, Kim MS, Kim S, *et al.* Highly sensitive, flexible, and wearable pressure sensor based on a giant piezocapacitive effect of three-dimensional microporous elastomeric dielectric layer. ACS Appl Mater Interfaces 2016;8:16922-31.
32. Kang S, Lee J, Lee S, Kim SG, Kim JK, Algadi H. Highly sensitive pressure sensor based on bioinspired porous structure for real time tactile sensing. Adv Electron Mater 2016;2:406-15. [doi: 10.1002/aelm. 201600356].
33. Kim KN, Lee JP, Lee SH, Lee SC, Baik JM. Ergonomically designed replaceable and multifunctional triboelectric nanogenerator for a uniform contact. RSC Adv 2016;6:88526-30.
34. Chen M, Zhang L, Duan S, Jing S, Jiang H, Li C. Highly stretchable conductors integrated with a conductive carbon nanotube/graphene network and 3D porous poly (dimethylsiloxane). Adv Funct Mater 2014;24:7548-56.
35. Yang C, Xu Y, Man P, Zhang H, Huo Y, Yang C, *et al*. Formation of large-area stretchable 3D graphene-nickel particle foams and their sensor applications. RSC Adv 2017;7:35016-26.
36. Yang L, Wang R, Song Q, Liu Y, Zhao Q, Shen Y. One-pot preparation of porous piezoresistive sensor with high strain sensitivity via emulsion-templated polymerization. Compos Part A Appl Sci Manuf 2017;101:95-198.
37. Li Q, Duan T, Shao J, Yu H. Fabrication method for structured porous polydimethylsiloxane (PDMS). J Mater Sci 2018;53:11873-82.
38. Dezhkam R, Shafiei Souderjani A, Shamloo A, Eskandarisani M, Mashhadian A. Numerical investigation of centrifugal passive cell separation in three types of serpentine microchannels and comparison with fixed platform. J Indust Eng Chem 2023;155-67. [doi: 10.1016/j.jiec. 2023.04.013].
39. Keumarsi MM, Oskouei PF, Dezhkam R, Shamloo A, Vatandoust F, Amiri HA. Numerical study of a double stair shaped dielectrophoresis channel for continuous on chip cell separation and lysis using finite element method. J Chromatogr A 2023;1696:204-15. [doi: 10.1016/j.chroma. 2023.463960].
40. Kheirkhah Barzoki A, Dezhkam R, Shamloo A. Tunable velocity based deterministic lateral displacement for efficient separation of particles in various size ranges. Phys Fluids 2023;35:309-18. [doi: 10.1063/5.0158777].
41. Momeni M, Shamloo A, Hasani-Gangaraj M, Dezhkam R. An experimental study of centrifugal microfluidic platforms for magnetic-inertial separation of circulating tumor cells using contraction-expansion and zigzag arrays. J Chromatogr A 2023;1706:464249.
42. Pellegrino M, Sciambi A, Treusch S, Durruthy-Durruthy R, Gokhale K, Jacob J, *et al.* High-throughput single-cell DNA sequencing of acute myeloid leukemia tumors with droplet microfluidics. Genome Res 2018;28:1345-52.
43. Xu L, Durruthy Durruthy R, Eastburn DJ, Pellegrino M, Shah O, Meyer E, *et al*. Clonal evolution and changes in two AML patients detected with a novel single cell DNA sequencing platform. Sci Rep 2019;9:184-196. [doi: 10.1038/s41598 019 47297 z.].
44. Hatami A, Saadatmand M. Extremely precise blood-plasma separation from whole blood on a centrifugal microfluidic disk (Lab-on-a-Disk) using separator gel. Diagnostics (Basel) 2022;12:2873.
45. Hatami A, Saadatmand M, Garshasbi M. Cell-free fetal DNA (cffDNA) extraction from whole blood by using a fully automatic centrifugal microfluidic device based on displacement of magnetic silica beads. Talanta 2024;267:125245.
46. Malakshah VM, Darabi M, Sattari A, Hanafizadeh P. Numerical investigation of double emulsion formation in non-Newtonian fluids using double co-flow geometry. Chem Eng Res Des 2024;23:165-77. [doi: 10.1016/j.cherd.2024.01.041].
47. Sattari A, Tasnim N, Hanafizadeh P, Hoorfar M. Numerical study of double emulsion droplet generation in a dual coaxial microfluidic device using response surface methodology. Chem Eng Process Process Intensification 2021;162:571-84. [doi: 10.1016/j.cep. 2021.108330].

48. Aliverdinia M, Eskandarisani M, Moghaddam EA, Zand MM, Dehkordi MR. Numerical Study of Particle Focusing and Concentration under the Effect of Acoustic Waves in a Microchannel. In: Institute of Electrical and Electronics Engineers (IEEE); 2023. p. 76-80.
49. Dezhkam R, Amiri HA, Collins DJ, Miansari M. Continuous submicron particle separation via vortex-enhanced ionic concentration polarization: A numerical investigation. Micromachines (Basel) 2022;13:2203.
50. Sani MM, Aliverdinia M, Zand MM. Numerical Study of Different Pillar Shapes Using Deterministic Lateral Displacement Method for Particle Separation. In: 2022 30th International Conference on Electrical Engineering, ICEE 2022, Institute of Electrical and Electronics Engineers Inc.; 2022. p. 469-73.
51. Aliverdinia M, Moghaddam EA, Eskandarisani M, Zand MM. Dielectrophoretic Separation of RBCs from Platelets: A Parametric Study. In: 2022 29th National and 7th International Iranian Conference on Biomedical Engineering (ICBME), IEEE; 2022. p. 51-7.
52. Lee BY, Kim J, Kim H, Kim C, Lee SD. Low-cost flexible pressure sensor based on dielectric elastomer film with micro-pores. Sens Actuators A Phys 2016;240:103-9.
53. Javidi R, Moghimi Zand M, Alizadeh Majd S. Designing wearable capacitive pressure sensors with arrangement of porous pyramidal microstructures. Micro and Nano Systems Letters 2023;11:13.